CONF-900466--57

DE90 012212

DEFORMATION AND FRACTURE BEHAVIOR OF TiAl

C. L. Fu and M. H. Yoo, Metals and Ceramics Division, Oak Ridge National Laboratory, P.O. Box 2008, Oak Ridge, TN 37831-6114.

ABSTRACT

First-principles total-energy calculations of the elastic constants, shear fault energies, and cleavage energies of TiAl are presented. We find a large elastic shear anisotropy along the [011] direction, and high APB energies due to the strong cohesion between Ti and Al layers. Shear faults of SISF, SESF, and twin boundary are predicted to be prevalent due to their low energies. The anomalous temperature dependence of flow stress is explained by the cross-slip pinning and fault dragging mechanisms. The intrinsic brittleness of TiAl is discussed in terms of the low mobility of 1/2[110] dislocations.

INTRODUCTION

TiAl has attractive properties for high temperature structural application. It has large elastic modulus, high melting point, and relatively low density. However, the lack of ductility has limited its application. TiAl is stabilized in the $L1_0$ structure with alternate Ti and Al layers stacking along the c-axis. Obviously, the $L1_0$ crystal structure has suggested the anisotropic characters of TiAl. The mechanical properties of TiAl are very intriguing. For instance, an anomalous (positive) temperature dependence of yield stress from room temperature up to a peak temperature at about 600°C has been observed by Kawabata et al.[1] Earlier, Lipsitt et al.[2] observed a sharp brittle-to-ductile transition near 1000K for TiAl under tensile strain. More recently, the deformation microstructures were characterized by Court et al.[3] using transmission electron microscopy (TEM) and the dislocation substructures were investigated by Hug et al.[4] using weak-beam TEM. It is observed that the dislocation microstructure is dominated by the glide of $[01\bar{1}]$ superdislocations on the (111) plane at low temperatures and these superdislocations are in the form of Kear-Wilsdorf lock at elevated temperatures. On the other hand, the increase in ductility is interpreted in terms of the increasing activity of 1/2[110] ordinary dislocations. In addition, ordered twinning of $[11\bar{2}](111)$ is also observed to be a dominant deformation mode in plastic deformation at high temperatures.

In order to understand the intrinsic brittleness at low temperature and the anomalous thermal strengthening effect, first-principles calculation using density functional band theory (full-potential linearized augmented plane-wave method)[5] has been combined with anisotropic elasticity theory for dislocations[6] to study the electronic structure and the dislocation reactions of TiAl. We have determined six independent elastic constants, various shear fault energies, and the cleavage energy for various crystallographic planes. We find large elastic shear anisotropy along the [011] direction due to the directional Ti-Al bond. The anomalous temperature dependence of flow stress is explained by the cross-slip pinning and fault dragging mechanisms of the [011] superdislocations. A mechanism

"The submitted manuscript has been authored by a contractor of the U.S. Government under contract No. DE-AC05-84OR21400. Accordingly, the U.S. Government retains a nonexclusive, royalty-free license to publish or reproduce the published form of this contribution, or allow others to do so, for U.S. Government purposes."

---

based on interaction torque can explain the physical source for the low mobility of 1/2[110] screw dislocations.

FIRST-PRINCIPLES TOTAL-ENERGY CALCULATIONS

The crystal structure of TiAl is face-centered tetragonal of the $L1_0$ type. On the basis of our first principles calculation, we obtained a ground state equilibrium unit cell volume (V_o) of 31.13 Å^3 with an axial ratio c/a = 1.01, which is in good agreement with experiments (V_o = 32.69 Å^3 and c/a = 1.02). For crystals with the $L1_0$ structure, there are six independent elastic constants. A set of six independent total-energy calculations (i.e. total energy as a function of strain) is necessary in order to determine these elastic constants. Among these, (C_{11}-C_{12}) corresponds to the [110] shear strain on the ($1\bar{1}0$) plane, C_{66} corresponds to the [100] shear strain on the (010) plane, ($C_{11} + C_{33} - 2C_{13}$) corresponds to the [011] shear strain on the ($0\bar{1}1$) plane, and C_{44} corresponds to the [010] shear strain on the (001) plane. In addition, we have determined bulk modulus and distortion energy of longitudinal elastic wave along the [001] direction. The sublattice relaxation terms do not contribute in the present case due to symmetry constraints. The shear elastic anisotropy factor is given by $A_1 = 2C_{66}/(C_{11}-C_{12})$ for the [110] shear and by $A_2 = 4C_{44}/(C_{11} + C_{33} - 2C_{13})$ for the [011] shear.

The calculated elastic constants and shear and Young's moduli (Hill's average) are given in Table I. It is interesting to note that there is a notable difference between C_{44} and C_{66} values, indicating the anisotropic character of atomic bonding between adjacent planes in different directions. The shear anisotropy factor is larger for the [011] shear direction due to a relatively high C_{44} value (A_1 = 1.18 and A_2 = 2.46).

TABLE I. ELASTIC CONSTANTS, SHEAR MODULUS (G), AND YOUNG'S MODULUS (E) OF TiAl (in units of $10^{11}N/m_2$)

	C_{11}	C_{33}	C_{12}	C_{13}	C_{44}	C_{66}	G	E
Theory	1.90	1.85	1.05	0.90	1.20	0.50	0.70	1.76
Exp.	Static (ref. 2)						0.71	1.78
	Dynamic (ref. 7)						0.70	1.74

For the calculations of planar stacking fault energies, we use a supercell total-energy approach by introducing periodic stacking faults.[8] The atomic relaxations near the faults are not included in this investigation. However, since Ti and Al have very similar atomic sizes, the relaxations near the faults are expected to be small. We find high APB energies on the (010) and (111) planes ($E_{APB}(100)$ = 430 mJ/m^2, $E_{APB}(111)$ = 510 mJ/m^2), and relatively low twinning, SISF, and SESF energies on the (111) plane with values 60 mJ/m^2, 90 mJ/m^2, and 80 mJ/m^2, respectively. Although there is a large discrepancy between the calculated and recently measured APB energies by Hug et al. ($E_{APB}(111) \approx 130\text{-}160$ mJ/m^2),[4] the high values of our calculated APB energy is consistent with the other theoretical estimates[9,10] and the earlier experimental observations that no APB's are discernible in TiAl.[1,9] The high APB energy is attributed to the directional bonding of Ti(d-electron) and Al(p-electron). By contrast, the boundary interface created by twinning does not change the Ti-Al or Ti-Ti nearest-neighbor bonding (the twinning energy comes from the change of bond angles between second-nearest-neighbors) and a lower boundary energy is expected. Locally, SISF and SESF can be viewed as "microtwins"; therefore, the values of the corresponding fault energies are very similar to that of twinning.

To gain an in-depth understanding of the bonding character of TiAl, we present in Fig. 1 the valence charge density contour plot on the (010) plane (i.e. a mixed Ti-Al plane) and on the (001) plane (i.e. a pure Ti plane). The charge distribution about Ti site is shown to be highly non-spherical and the orbital character is dominated by d_{xy}, d_{xz} and d_{yz} components. The existence of Ti directional bonds in the (001) Ti layer may hinder the generation (and the mobility) of 1/2[110] dislocations. Furthermore, we find a p_z-type charge polarization about the Al site, indicating strong cohesion between Ti and Al layers. The directional bonding of Ti(d-electron) and Al (p-electrons) is manifested in a large C_{44} value (since the corresponding shear deformation involves shear between pure Ti and pure Al layers) and a high APB energy. In fact, it may well be this Ti-Al directional bond which causes this alloy to be brittle. A similar conclusion has been suggested recently by Morinaga et al.[11] from their electronic structure calculation of a TiAl cluster. Our result is markedly different from that of Greenberg et al.[12] in that we find the strong directional character of the Al p-electron to play an important role in the strong cohesion between Ti and Al layers.

For the cleavage energy calculation, we consider three crystallographic planes, i.e., (110), (100), and (001). We model the surface by single-slab geometry. The cleavage

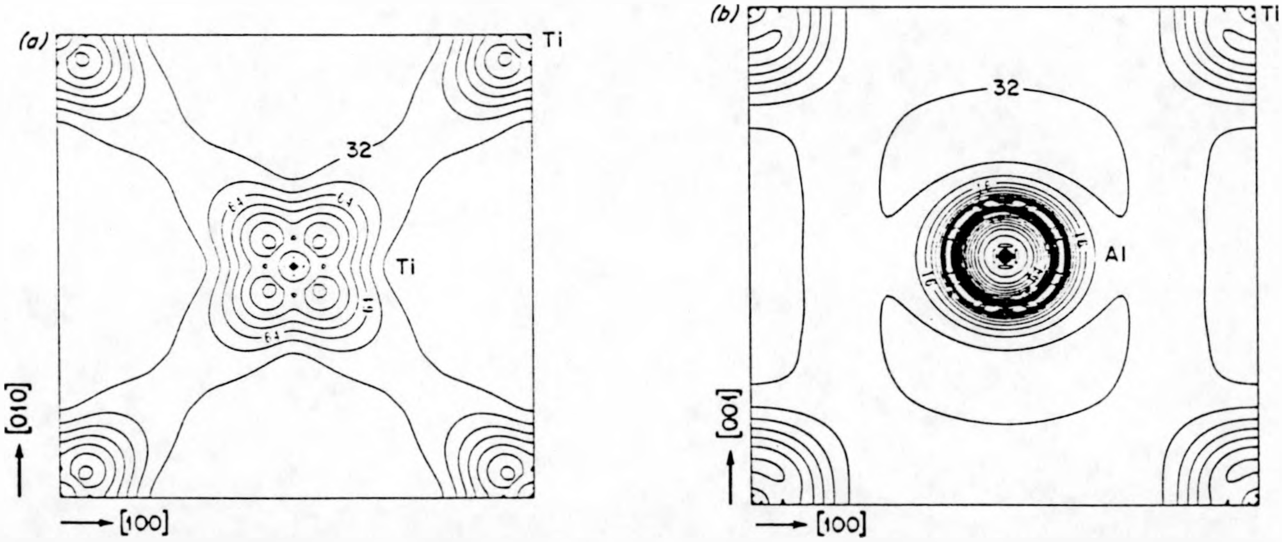

Fig. 1. Valence charge density contour plots in the (a) pure Ti (001) plane, and (b) mixed Ti-Al (010) plane in units of $10^{-3}e/(a.u.)^3$

energy, defined as the energy required to separate the solid into two semi-infinite crystals, can be determined by comparing the total energy of the slabs with that of bulk crystal. No surface relaxation or surface reconstructions are included in the present calculation. We find cleavage energy of 5.3 and 5.6 J/m^2 for the (110) and (001) planes, respectively (both planes are terminated by either pure Ti or pure Al layer). The cleavage energy of (100) plane (which is terminated by a mixed Ti-Al layer) is found to be 4.6 J/m.^{2} The cleavage plane of TiAl is predicted to be the mixed Ti-Al plane from the point of view of ideal cleavage strength.

The theoretical cleavage energy of TiAl is comparable to that of Ni_3Al and much higher than those of trialuminides.[13] It is apparent that the brittle fracture of TiAl at low temperature is not caused by the intrinsic low cleavage strength. The lack of plastic work due to the low mobility of 1/2[110] dislocations (see below for discussion) to shield the crack tip is the main cause for the low ductility of this alloy. As an example of the importance of plastic work, we have made an analysis of the orientation dependence of the crack tip plasticity by slip and twinning by considering (110) and (001) cracks.[14] We find that the elastic shear strain associated with slip and twinning near the (110) crack is larger than that near the (001) crack. Given the fact that the difference in the cleavage energy between the (110) and (001) planes is very small (i.e., only about 5%), it may be concluded that the effectiveness for localized slip and twinning to stop the (110) slip is higher than to stop the (001) crack. Our prediction is consistent with the experimental result by Kawabata et al..[15]

DISLOCATION MICROSTRUCTURES

1/2[110] Ordinary Dislocations

Court et al.[3] attributed the brittle-to-ductile transition to the increase in mobility of 1/2[110] dislocations at high temperatures. It is generally recognized that the activation of 1/2[110] can provide four independent shears to ensure the strain compatibility. On the other hand, noting the conjugate relationship between the complementary $[\bar{1}\bar{1}2](111)$ twinning and the ordinary 1/2[110] slip, Yoo[16] suggested that increasing propensity of both the ordered twinning and the ordinary slip is the main cause for the observed brittle-to-ductile transition.

Energetically, the 1/2[110] dislocations can be dissociated into 1/6[121] and $1/6[21\bar{1}]$ partials by forming complex stacking fault (CSF) ribbons on the $(1\bar{1}1)$ plane. The interaction between these partials determines the mobility of 1/2[110] dislocation. We model the interaction between partials using anisotropic elasticity theory for dislocations[6] in conjunction with the elastic constants determined from first-principles. For the [110] $(1\bar{1}1)$ screw configuration, we find a large interaction torque acting on individual partials with a ratio $f_\theta/f_r=1.5$, where f_r and f_θ are the radial and angular force constant, respectively. A large interaction torque implies a non-planar dislocation core structure, which can give rise to the glide resistance of 1/2[110] dislocation on the $(1\bar{1}1)$ plane. On the other hand, the interaction torque vanishes (by symmetry) for the $[110](1\bar{1}1)$ edge configuration.

Our result indicates that 1/2[110] dislocation is sessile at low (and room) temperatures. Furthermore, we predict a long screw configuration for 1/2[110] dislocation under stress due to the low mobility of its screw part. Analysis shows that the large interaction torque term originates from the large anisotropy A_2 factor, which is related to the directional Ti-Al bond.

Three-fold Dissociation of [011] Superdislocations and Anomalous Thermal Strengthening Effect

According to Hug et al.^{4} the dissociation of superdislocation of [011] Burgers vector proceeds from [011] → 1/2[011] + 1/6[121] + 1/6[$\bar{1}$12] by forming two parallel strips of APB and SISF ribbons on the (1$\bar{1}$1) plane. A schematic drawing of the three-fold dissociation is shown in Fig. 2 for the case of screw dislocation. The equilibrium widths of APB and SISF ribbons are calculated by using the radial components of pair-wise interaction forces^{17} among the three partial dislocations and the calculated APB and SISF energies. We find fault widths of 0.8 nm (screw) and 1.4 nm (edge) for the APB ribbon and 5.0 nm (screw) and 9.0 nm (edge) for the SISF ribbons. Our result is markedly different from that of Hug et al.^{4} in that the APB widths are far smaller in our case. The sources for the discrepancy are unclear at present. Our result favors an extremely narrow (or marginally indiscernible by TEM) APB for this alloy.

Despite its narrow ribbon, the existence of APB plays a vital role in the thermal strengthening mechanism of TiAl. In Fig. 2 we also show the schematic cross-section of the three-fold dissociation, including the net tangential force at each dislocation core. While these forces add up to zero, the net moment (i.e. torque) at each dislocation core

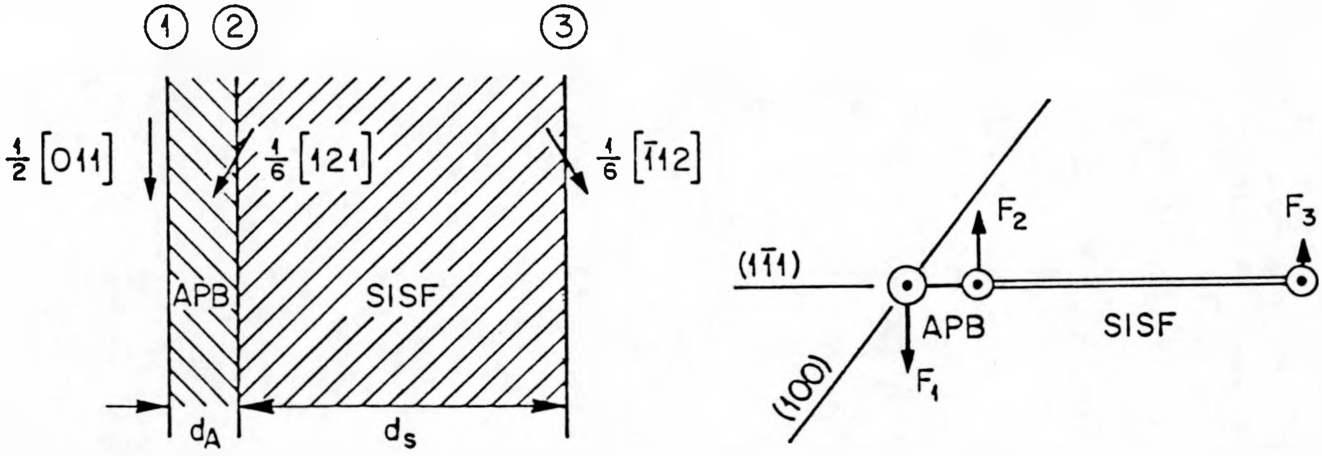

Fig. 2. Three-fold dissociations of an [011] superdislocation on the (1$\bar{1}$1) plane. $\vec{F}_1 = -112$, $\vec{F}_2 = 88$, and $\vec{F}_3 = 24$ in units of mJ/m.

is finite. As a result, when a screw superdislocation moves to the left on the $(1\bar{1}1)$ plane (see Fig. 2) under the resolved shear stress, the torque exerted by $\vec{F}_1 = -112$ mJ/m and $\vec{F}_2 = 88$ mJ/m can assist the kink-pair formation onto the (100) plane, thus facilitating the cross-slip-pinning mechanism.[17] When, on the other hand, the sign of the resolved shear stress is reversed such that the dislocation moves to the right (see Fig. 2), the mobility of trailing dislocations (1 and 2) would be reduced as compared to that of the leading one (3). Therefore, owing to the interaction torque, all [011] screw superdislocations in TiAl are capable of cross-slip pinning or SISF-dragging depending on the sense of the resolved shear stress. While the cross-slip pinning may be responsible for the yield strength anomaly, the SISF-dragging with an appropriate multiplication mechanism may lead to nucleation of a twin.

ACKNOWLEDGEMENT

Research sponsored by the Division of Materials Sciences, Office of Basic Energy Sciences, U.S. Department of Energy, under contract DE-AC05-84OR21400 with Martin Marietta Energy Systems, Inc.

REFERENCES

1. T. Kawabata, T. Kania, and O. Izumi, Acta Metall. 33, 1355 (1985).
2. H. A. Lipsitt, D. Shechtman, R. E. Schafrik, Metall. Trans. 6A, 1991 (1975).
3. S. A. Court, V. K. Vasudevan, and H. L. Fraser, Phil. Mag. A61, 141 (1990).
4. G. Hug, A. Loiseau, and P. Veyssiere, Phil. Mag. A57, 499 (1988).
5. E. Wimmer, H. Krakauer, M. Weinert, and A. J. Freeman, Phys. Rev. B24, 864 (1981); C. L. Fu, M. Weinert, and A. J. Freeman (to be published).
6. A. N. Stroh, Phil. Mag. 3, 625 (1958).
7. R. E. Schafrik, Metall. Trans. 8A, 1003 (1977).
8. C. L. Fu and M. H. Yoo, Mat. Res. Soc. Symp. Proc. 133, 81 (1989).
9. D. Shechtman, M. J. Blackburn, and H. A. Lipsitt, Metall. Trans. 5, 2 (1974).
10. M. Yamaguchi, Y. Umakoshi, and T. Yamane, in Dislocations in Solids (University of Tokyo), 77 (1985).
11. M. Morinaga, J. Saito, N. Yukawa, and H. Adachi, Acta Metall. (1990).
12. B. F. Greenberg, V. I. Anisimov, and Yu N. Gornostrirev, Scripta Metall. 22, 859 (1988).
13. C. L. Fu, J. of Mater. Res. 5, 971 (1990).
14. M. H. Yoo, C. L. Fu, and J. K. Lee, Mat. Res. Soc. Symp. Proc. 133, 189 (1989).
15. T. Kawabata, Y. Takezono, T. Kanai, and O. Izumi, Acta Metall. 36, 963 (1988).
16. M. H. Yoo, J. Mater. Res. 4, 50 (1989).
17. M. H. Yoo, Scripta Metall. 20, 915 (1986); Acta Metall. 35, 1559 (1987).